Photocatalytic degradation of gaseous benzene over TiO$_2$/Sr$_2$CeO$_4$: Kinetic model and degradation mechanisms

Junbo Zhong, Jianli Wang, Lin Tao, Maochu Gong, Liu Zhimin, Yaoqiang Chen *

College of Chemistry, Sichuan University, Sichuan 610064, PR China

Abstract

Photocatalytic oxidation of benzene in air was carried out over TiO$_2$/Sr$_2$CeO$_4$ catalysts. The prepared photocatalyst was characterized by S_{BET}, UV–vis diffuse reflectance and XPS. TiO$_2$/Sr$_2$CeO$_4$ absorbs much more visible light than TiO$_2$ in the visible light region. The XPS spectrum shows that the binding energy value of Ti 2p$_{3/2}$ transfers to a lower value. The main purpose was to investigate the kinetic model and degradation mechanisms. The kinetic data matched well with the Langmuir–Hinshelwood (L–H) kinetic model with the limiting rate constant and the adsorption constant in this case were 0.0064 mg l^{-1} min^{-1} and 9.20781 mg^{-1}, respectively. No gas-phase intermediates were detected by direct GC/FID analysis under the conditions despite the high benzene concentration. Ethyl acetate and (3-methyl-oxiran-2-yl)-methanol were two major identified intermediates which were accompanied by butylated hydroxytoluene, 2,6-bis(1,1-dimethylethyl)-4,4-dimethylycyclohe, 2,5-cyclohexadiene-1,4,dione,2,6-bis(1,1-dim). It is plausible that at least one of these less-reactive intermediates caused the deactivation of the photocatalyst. Finally, the photocatalytic oxidation mechanisms were speculated.
© 2006 Elsevier B.V. All rights reserved.

Keywords: TiO$_2$; Benzene; Kinetic; Photocatalytic degradation

1. Introduction

At present, the widespread applications of volatile organic compounds (VOCs) in industrial process and domestic activities have led to water and air pollution, particularly a serious consequence if takes place in indoor surroundings. Many VOCs are considered to be toxic and carcinogenic. The most significant problem related to the emission of VOCs is focused on the potential production of photochemical oxidants; for example, ozone and peroxyacetyl nitrate [1].

Among the technologies developed for the treatment of VOCs, the photocatalytic oxidation process (AOP) is considered to be a promising technology. AOP is initiated from the generation of electron–hole pairs on the semiconductor upon absorbing ultraviolet light with energy which is equal to or higher than the band gap energy. Electrons and holes photogenerate in the bulk of the semiconductor and move to the particle surface, electrons reduce electron acceptors such as molecular oxygen, and hole can oxidize electron donors including absorbed water or hydroxide anion to give hydroxyl radicals [2].

The decomposition of volatile organic compounds has been difficult because of the low conversion and the common deactivation of photocatalyst. Therefore it is crucial to prolong the lifetime of the photocatalyst and enhance its photocatalytic activity. Various techniques have been developed for development and modification of the TiO$_2$-based photocatalysts [3].

The TiO$_2$ photocatalytic oxidation of benzene has been studied by several authors [4–19]. Wang and co-workers reported that decomposition of benzene in air streams by UV/TiO$_2$ process can be adequately described by using the Langmuir–Hinshelwood (L–H) kinetic model [7]. Analysis of the products recovered from used TiO$_2$ can provide information for the degradation mechanisms. Concerning degradation mechanisms, the benzyl radical has been suggested to be the key species at origin of the formation of benzyl alcohol and benzaldehyde [20]. d'Hennezel and co-workers reported that the major by-products of benzene was phenol which was accompanied by hydroquinone and 1,4-benzoquinone. Wang noted phenol was identified to be the major intermediate generated at the early

* Corresponding author. Tel.: +86 28 85418451; fax: +86 28 85418451.
E-mail addresses: zhongjunbo@sohu.com, scuzhong@sina.com (J. Zhong), liuzhimin2648@sina.com (L. Zhimin).

Nomenclature

k	reaction rate constant ($mg\,l^{-1}\,min^{-1}$)
K	adsorption equilibrium constant ($l\,mg^{-1}$)
k_{obs}	observed pseudo first-order rate constant
R	interrelated coefficients
RH	relative humidity (%)
r_0	initial photocatalytic degradation rate ($mg\,l^{-1}\,min^{-1}$)
t	reaction time (min)
$t_{0.5}$	half-life of gaseous benzene (min)

Greek symbols

ρ	concentration of gaseous benzene at moment ($mg\,l^{-1}$)
ρ_0	initial concentration of gaseous benzene ($mg\,l^{-1}$)

stage of benzene decomposition and the final products were found to be CO_2, CO, H_2O [4]. Other researchers argued that the intermediates adsorbed on TiO_2 for the photocatalytic oxidation of benzene were identified to be phenol, maloinic acid, hydroquinone, benzoic acid and benzoquinone [18,19].

Sr_2CeO_4 is blue–white phosphor, it can exhibit photoluminescence under excitation with irradiation of ultraviolet rays [21]. The excitation spectra present two broad bands with maxima at 280 and 340 nm and the emission spectrum has a broad band centered at 465 nm [22]. In order to prolong the lifetime of photocatalyst and enhance its photocatalytic activity, TiO_2 was coated onto the fluorescent material Sr_2CeO_4.

However, to our knowledge, study on kinetic model and degradation mechanisms of gaseous benzene over TiO_2/Sr_2CeO_4 has not been reported. In the present work, the kinetics of photocatalytic degradation of benzene in the gas phase over TiO_2/Sr_2CeO_4 was closely studied. The Langmuir–Hinshelwood (L–H) kinetics was successfully applied to describe the heterogeneous gas solid reaction, and the initial reaction rate and its relating factors were emphasized. Simultaneously, the reaction products adhered on the deactivated TiO_2/Sr_2CeO_4 were identified by FT-IR or GC/MS. On the basis of these analyses, the degradation mechanisms were speculated.

2. Experimental

2.1. Preparation of TiO₂/Sr₂CeO₄

The $SrCO_3$ and CeO_2 (AR, Kelong Co. Ltd.) were mixed with a nominal composition of Sr_2CeO_4, and was finely ground in agate mortar for 1 h and fired at 1273 K for 4 h in muffle furnace in air. Finally, the Sr_2CeO_4 superfine particles were obtained.

Precursor solution for TiO_2 was prepared by the following method. Tetrabutylorthotitanate (17.2 ml) and diethanolamine (4.8 ml) were dissolved in ethanol (67.28 ml). After stirring vigorously for 2 h at room temperature, a mixed solution of deionized water (0.9 ml) and ethanol (10 ml) was added dropwise to the above solution with a burette under stirring. The resultant

alkoxide solution was kept at room temperature for hydrolysis reaction for 2 h, until the TiO_2 sol formed. The composition ratio of $Ti(OC_4H_9)_4$, C_2H_5OH, H_2O and $NH(C_2H_4OH)_2$ in the starting alkoxide solution was 1:26.5:1:1 (in molar ratio). The pure TiO_2 power was prepared after calcination the TiO_2 gel at 773 K.

The photocatalyst of TiO_2/Sr_2CeO_4 with loading amount of TiO_2 (1 wt.%) was prepared by impregnating method using TiO_2 sol, then calcinated at 773 K for 2 h.

2.2. Charaterization of TiO₂/Sr₂CeO₄

Surface area analysis of TiO_2/Sr_2CeO_4 and TiO_2 was carried out by the Brunauer–Emmet–Teller (BET) method using Autosorb-ZXF-05 (Xibei Chemical Institute, China). XPS measurement was carried out on a spectrometer (XSAM-800, KRATOS Co.) with Mg Kα anticathode. The UV–vis diffuse reflectance spectrum was performed on a spectrometer (TU-1907). Deactivated TiO_2/Sr_2CeO_4 catalyst samples were characterized by a FT-IR (16PC). Adsorbed intermediates were extracted from the deactivated TiO_2/Sr_2CeO_4 samples by ether and ultrasonication. Qualitative analysis of the filtrate was carried on the 6890N GC-5973 MS (Agilent Co.) with chemical structure analytic software.

2.3. Procedure

Experiments were carried out in a closed stainless steel reactor with the volume of 105 l. An electric fan and three 10 W germicidal lamps with the maximum wavelength of 253.7 nm were installed on a bracket (see Fig. 1). Photocatalyst powder with 20 g was dispersed in a thin layer over two aluminum foils with the total area of 980 cm^2, and the required quantity of liquid benzene was injected into the reactor and once dark-adsorption equilibrium had been reached, photocatalysis was started by turning on the UV light source. The photocatalytic oxidation of benzene was performed under illumination at 312–31 K to avoid condensation of benzene by placing two infrared lamps outside the reactor to heated. The concentration of benzene was
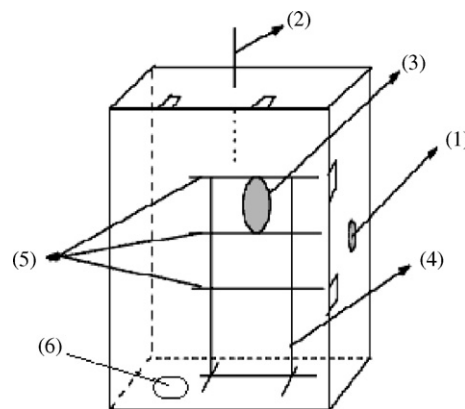

Fig. 1. Schematic diagram of the batch photocatalytic reactor: (1) sampling point; (2) thermometer; (3) electric fan; (4) bracket; (5) germicidal lamp; (6) hygrometer.
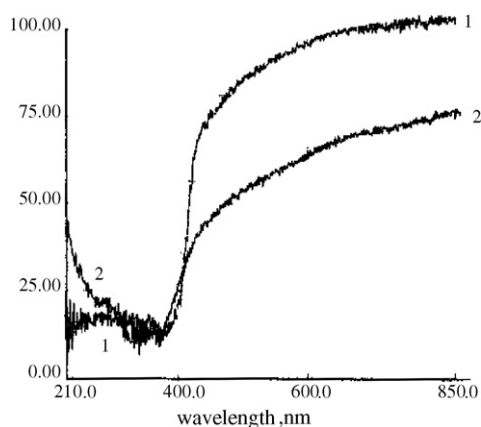
Fig. 2. UV–vis diffuse reflectance spectra: (1) TiO$_2$; (2) TiO$_2$/Sr$_2$CeO$_4$ (1.0 wt.%).

detected by the gas-phase chromatogram with FID detector and GDX-101 chromapack column. The gas was withdrawn regularly from the reactor for analysis.

3. Results and discussion

3.1. Characterization of the catalyst

Since the pure and loaded titania samples were prepared for use in the photocatalytic reaction, their UV–vis diffuse reflective properties may have had a strong effect on the photocatalytic activity. Fig. 2 shows the diffuse reflectance spectrum of pure and loaded TiO$_2$.

As shown in Fig. 2, from 210 to 300 nm, two spectra have an obvious difference, TiO$_2$/Sr$_2$CeO$_4$ reflects much more ultraviolet light than TiO$_2$, which indicates that TiO$_2$ absorbs much more ultraviolet light than TiO$_2$/Sr$_2$CeO$_4$. It is plausible that Sr$_2$CeO$_4$ reflects a portion of ultraviolet light. From 300 to 400 nm, there is no difference between the two spectra. However, the presence of Sr$_2$CeO$_4$ clearly changes the spectra of TiO$_2$ in the visible light regions, TiO$_2$/Sr$_2$CeO$_4$ absorbs much more visible light than TiO$_2$. The results show that TiO$_2$/Sr$_2$CeO$_4$ can be excited by visible light.

The high resolution XPS spectrum corresponding to the surface of TiO$_2$ was characterized by a main doublet composed of two symmetric peaks situated at E_b(Ti 2p$_{3/2}$) = 458.9 eV and E_b(Ti 2p$_{1/2}$) = 464.6 eV (Table 1), the binding energy difference, $\Delta E_b = E_b$(Ti 2p$_{1/2}$) − E_b(Ti 2p$_{3/2}$) was 5.7 eV, as previously reported in the literature [23], but as for TiO$_2$/Sr$_2$CeO$_4$, only E_b(Ti 2p$_{3/2}$) = 458.2 eV was detected, no E_b(Ti 2p$_{1/2}$) was observed. Compared with pure TiO$_2$, the E_b(Ti 2p$_{3/2}$) of TiO$_2$/Sr$_2$CeO$_4$ is transferred to a lower value, the result indi-

cates that Ti forms strong radical links through oxygen bridges with Sr$_2$CeO$_4$. So it is obvious that there is stronger interaction between Sr$_2$CeO$_4$ and TiO$_2$.

3.2. Blank experiments

The contrast experiments were carried out under two different conditions: one with illumination but no catalyst, the other with TiO$_2$ (pure and loaded TiO$_2$) but no illumination. The results showed that the concentration of benzene (1 mg l^{-1}) kept the same under the former condition, while under the later case changed so little that could be ignored (during 4 h time period). The blank tests proved that the benzene rings are stable. Without illumination or photocatalyst, benzene is kinetically stable. It was also suggested that dark adsorption–desorption for benzene from gas phase was small; therefore the adsorption equilibrium could be established quickly.

3.3. Comparison photoactivity of TiO$_2$/Sr$_2$CeO$_4$ and TiO$_2$

The photocatalytic activity of TiO$_2$/Sr$_2$CeO$_4$ (S_{BET} is 20.08 m^2/g) and TiO$_2$ (S_{BET} is 76.68 m^2/g) was compared and presented in Fig. 3.

As shown in Fig. 3, in the process of decomposing, the pure TiO$_2$ deactivates after 2 h, and the maximum conversion of 32.0% is reached after 2 h, while for the 1.0 wt.% loaded catalyst, in the whole process of reaction, the conversion rate keeps increasing until 4 h when the photocatalytic activity begins to decline and the maximum conversion of 65.0% is reached. It is seen that the TiO$_2$ loaded on Sr$_2$CeO$_4$ can prolong the life of photocatalyst and enhance the photocatalytic activity of catalyst. It is plausible that stronger photocatalytic activity of TiO$_2$/Sr$_2$CeO$_4$ result from two factors.

The first factor is that the presence of Sr$_2$CeO$_4$ can prolong the life of electron–hole pairs and press the recombine of electron–hole pairs. Since the Sr$_2$CeO$_4$ compound posses one-dimensional chain of edge-sharing CeO$_6$ octahedra, in which the cerium ion is in the 4+ state and the 4f shell is empty. The blue luminescence from Sr$_2$CeO$_4$ was suggested from a ligand
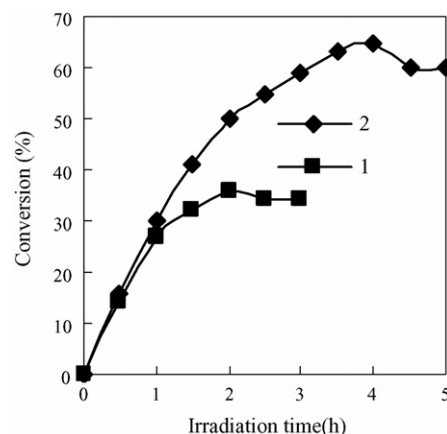
Table 1
Peak fitting results of the high resolution spectra of the Ti 2p

Sample	Ti 2p		
	E_b(Ti 2p$_{1/2}$)	E_b(Ti 2p$_{3/2}$)	ΔE_b
TiO$_2$	464.6	458.9	5.7
TiO$_2$/Sr$_2$CeO$_4$	–	458.2	–

Fig. 3. Conversion of benzene vs. irradiation time: (1) TiO$_2$ (0.2 g); (2) TiO$_2$/Sr$_2$CeO$_4$; relate humidity (RH): 50%.

O^{2-}-to-metal Ce^{4+} charge transfer [21]. Considering that an electron can be transferred from an oxygen ligand to the empty 4f shell of Ce^{4+}, a high spin triplet excited state is formed via a spinforbidden transfer. Therefore, the photoluminescence of Sr_2CeO_4 can be assigned to a ligand O^{2-}-to-metal Ce^{4+} transfer transition of Ce^{4+}[21,24]. In the present paper, Sr_2CeO_4 was used as support, TiO_2 was loaded on the surface of Sr_2CeO_4, when TiO_2 absorbs photons (recall the light with the maximum wavelength of 253.7 nm), electrons are excited from the valence to the conduction band leaving holes behind. When Sr_2CeO_4 absorbs ultraviolet ray, ligand O^{2-}-to-metal Ce^{4+} charge transfer forms, it will emits blue light, if the excited electron of TiO_2 transfer to ligand O^{2-} or metal Ce^{4+}, thus the recombine of electron–hole pairs can be pressed, which result in promotion the photocatalytic activity of TiO_2. The electron transfer mechanism is shown in Fig. 7.

The second factor is TiO_2/Sr_2CeO_4 increases the absorption in the region 400–850 nm. The emission spectrum of Sr_2CeO_4 has a broad band centered at 465 nm [22], the light emitted by Sr_2CeO_4 can excite TiO_2, thus the photocatalytic activity can be promoted.

From the above discussion, it is clearly that the two factors have a synergy which increases the photocatalytic activity of TiO_2/Sr_2CeO_4.

Since the TiO_2 loaded on Sr_2CeO_4 can prolong the life of photocatalyst and enhance the photocatalytic activity of catalyst, so it is possible and necessary to investigate the kinetic model and degradation mechanisms of gaseous benzene over TiO_2/Sr_2CeO_4.

3.4. Kinetics on the destruction of benzene

In typical experiments with benzene, the degradation of benzene started from various concentrations.

Fig. 4 is a plot of normalized concentration versus irradiation time for benzene at five different concentrations. The logarithmic transforms for these concentration curves are shown in Fig. 5. The degradation rates fit a first-order model well, namely, the integral equation of $\ln(\rho_0/\rho_t) = k_{obs}t$ describes the tendency well, where ρ_0 and ρ_t are the concentration of benzene at the point of time 0 and t, respectively, and k_{obs} is the observed pseudo first-order rate constant. The slop of a liner plot of $\ln(\rho_0/\rho_t)$ versus time gives the apparent degradation rate constant. To make the further mathematic inferences clear, all the relating kinetic parameters, such as the reaction rate constants (k_{obs}), half-life ($t_{0.5}$), calculated initial reaction rate (r_0) and interrelated coefficients (R) of the lines in Fig. 5 are all presented in
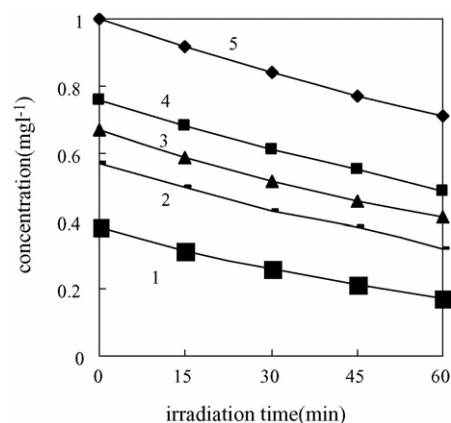

Fig. 4. Plot of photo-degradation of benzene vs. irradiation time, at various initial concentration of benzene: from bottom to top (1) 0.38 mg l^{-1}; (2) 0.57 mg l^{-1}; (3) 0.67 mg l^{-1}; (4) 0.76 mg l^{-1}; (5) 1.0 mg l^{-1}; RH: 50%.
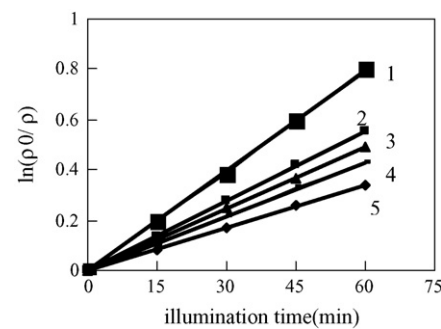

Fig. 5. $\ln(\rho_0/\rho)$ vs. illumination time. Initial concentration of benzene: from top to bottom (1) 0.38 mg l^{-1}; (2) 0.57 mg l^{-1}; (3) 0.67 mg l^{-1}; (4) 0.76 mg l^{-1}; (5) 1.0 mg l^{-1}.

Table 2. That the decrease of k_{obs} as increasing the initial benzene concentration indicates that there is a competition between the intermediates and benzene for the active sites on the surface of catalyst. This can be confirmed from the deactivation of the catalyst. Considering the results above, the adsorption process can be excluded from the rate-determining step; hence the surface reaction is probably the rate-determining step.

Owing to the complex mechanism of reactions, it is difficult to develop a model for the dependence of the photocatalytic degradation rate on the experimental parameters for the whole treatment time. Thus, kinetic modeling of the photocatalytic process is usually restricted to the analysis of the initial rate of photocatalytic degradation. This can be obtained from the initial slope to the curves and the initial concentration in an experiment in which the variation of the concentration is measured

Table 2
Relating kinetic parameters on the photo-degradation of benzene

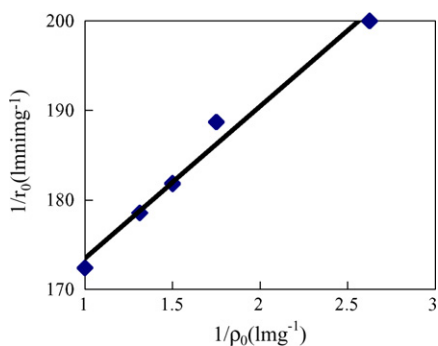| ρ_0 (mg l^{-1})	$1/\rho_0$ (l mg^{-1})	K (min^{-1})	$t_{0.5}$ (min)	R	r_0 (mg l^{-1} min^{-1})	$1/r_0$ (l min mg^{-1})
0.3809	2.6254	0.0132	52.5111	0.9998	0.0050	200.00
0.5714	1.7500	0.0093	74.5319	0.9982	0.0053	188.68
0.6667	1.4999	0.0082	84.5301	0.9996	0.0055	181.82
0.7619	1.3125	0.0073	94.9517	0.9997	0.0056	178.57
1.00	1.0000	0.0058	119.5081	0.9994	0.0058	172.41

Fig. 6. The linear transformation of $1/r_0$ vs. $1/\rho_0$.

as a function of time. The extrapolation of the photocatalytic degradation rate to time = 0 avoids the possible interference from by-products. The initial photocatalytic degradation rate (r_0) is observed to be a function of the initial concentration (ρ_0). A linear plot of r_0^{-1} versus ρ_0^{-1} is often obtained, and that gives k as the L–H rate constant and K as the Langmuir adsorption constant of the VOCs in the photocatalytic degradation reaction [13]:

$$r_0 = -\frac{d\rho}{dt} = \frac{kK\rho_0}{1 + K\rho_0}$$

The equation is further expressed in a linear form

$$\frac{1}{r_0} = \frac{1}{k} = \frac{1}{kK\rho_0}$$

The kinetic parameters k and K are obtained by using linear least squares analysis (see Fig. 6). The value of k and K are $0.0064\,mg\,l^{-1}\,min^{-1}$ and $9.2078\,l\,mg^{-1}$, respectively. Using the same analysis method, the value of k and K over 0.2 g pure TiO_2 are $0.0064\,mg\,l^{-1}\,min^{-1}$ and $4.6719\,l\,mg^{-1}$, respectively ($R = 0.9988$). So it is obvious that photocatalytic degradation of benzene on TiO_2/Sr_2CeO_4 and pure TiO_2 both match
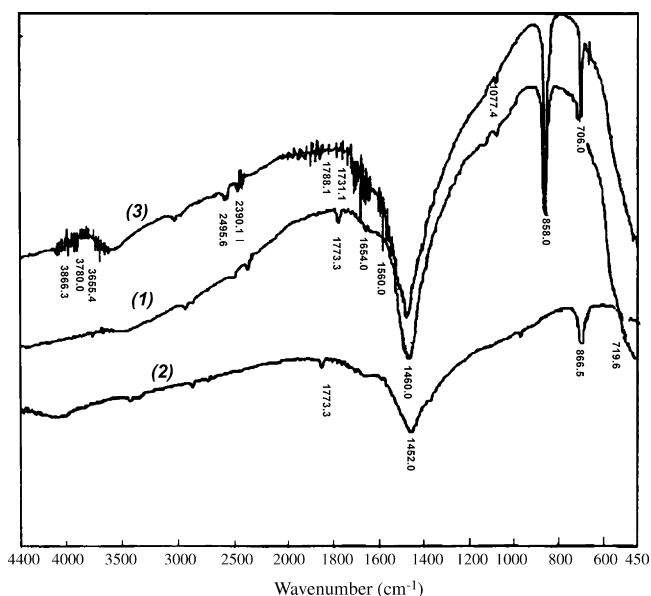

Fig. 7. FT-IR spectrum of TiO_2/Sr_2CeO_4: (1) fresh; (2) used 2 h; (3) used 4 h (deactivated) initial concentration of benzene was $1\,mg\,l^{-1}$.
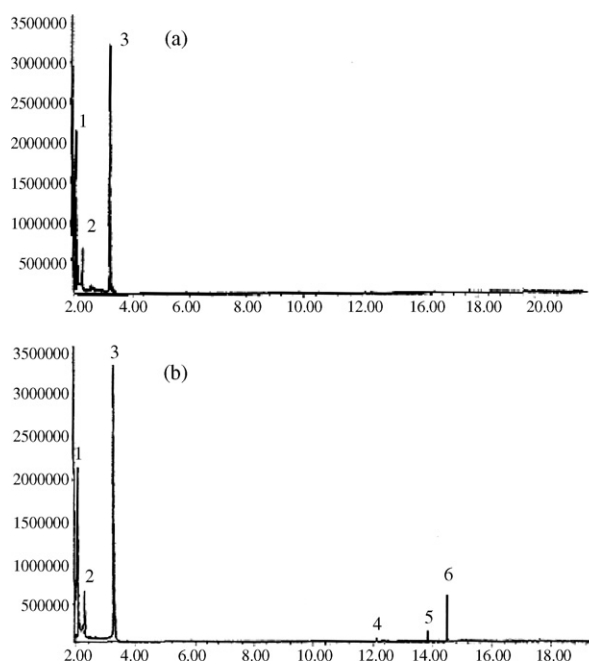

Fig. 8. Total chromatogram of intermediates from TiO_2/Sr_2CeO_4 detected by GC–MS: (a) used 2 h; (b) used 4 h (deactivated) initial concentration of benzene was $1\,mg\,l^{-1}$.

Langmuir–Hinshelwood (L–H) kinetic model. It is easy to under this point because both photocatalysts can generate hydroxyl radicals irradiated by UV under the same condition.

According to the discussions above, a mechanism based on the L–H kinetic model is advanced here: the photocatalytic degradation of benzene on the TiO_2/Sr_2CeO_4 follows three steps: (1) the adsorption of benzene molecules onto the surface
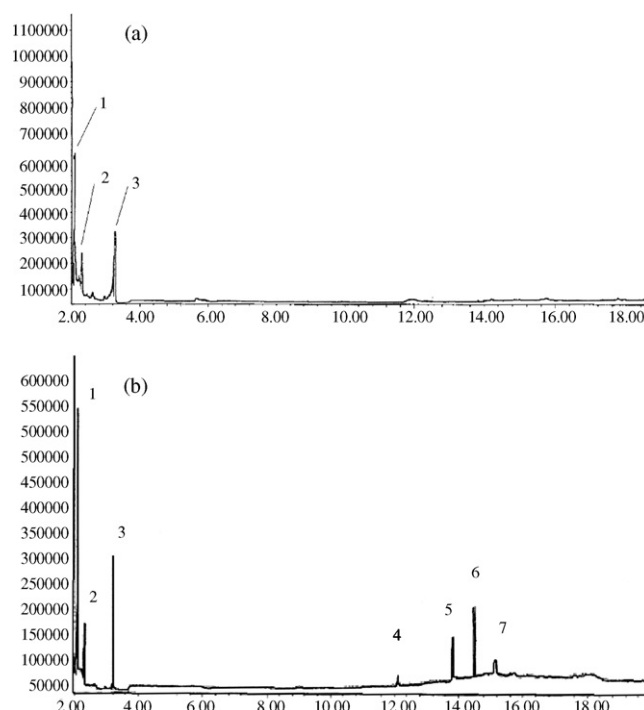

Fig. 9. Total chromatogram of intermediates from TiO_2 detected by GC–MS: (a) used 1 h; (b) used 2 h (deactivated) initial concentration of benzene was $1\,mg\,l^{-1}$.

of TiO$_2$/Sr$_2$CeO$_4$; (2) a fast inducement by the irradiation, which includes the produce of electron–hole pairs, hydroxyl radicals and likely oxidation; (3) the opening of benzene rings during the surface redox reactions. These steps can be further confirmed by the intermediates investigation. Actually, L–H kinetic model has successfully described many similar photocatalytic systems [8,15,25–28].

3.4.1. FT-IR investigation during photocatalytic oxidation

The objective of infrared experiments was to identify the adsorbed reaction intermediates and products adsorbed on the catalyst surface during photocatalytic oxidation. In general, such information can provide a vital understanding of the mechanism.

The chemical species adsorbed on the surface of photocatalyst were scanned by a FT-IR spectroscopy in the range of 450–4400 cm^{-1}. As shown in Fig. 7, no new bands appear on the surface of TiO$_2$/Sr$_2$CeO$_4$ used 2 h, which indicates that the photocatalyst has not been deactivated, thus it is reasonable

to investigate the kinetic model at the initial time. The band that in the region of 1500–1600 cm^{-1} in the spectrum (3) are related to C–H bonding and C=C bonding, respectively, and could be assigned to the signals of benzene derivatives and possibly oxidized aromatic intermediates. A strong absorbance shown between 1650 and 1780 cm^{-1} indicates the formation of C=O bonding, implying that the occurrence of the attack by the activated oxygen species or hydroxyl radical (OH$^\bullet$) upon the carbon structures. During the region of higher wave number (cm^{-1}), the bands in the region of 3600–3800 cm^{-1} could be assigned to the OH bonding of butylated hydroxytoluene and alcohols, which were believed to be intermediates form in various stages of reaction.

3.5. Benzene intermediates

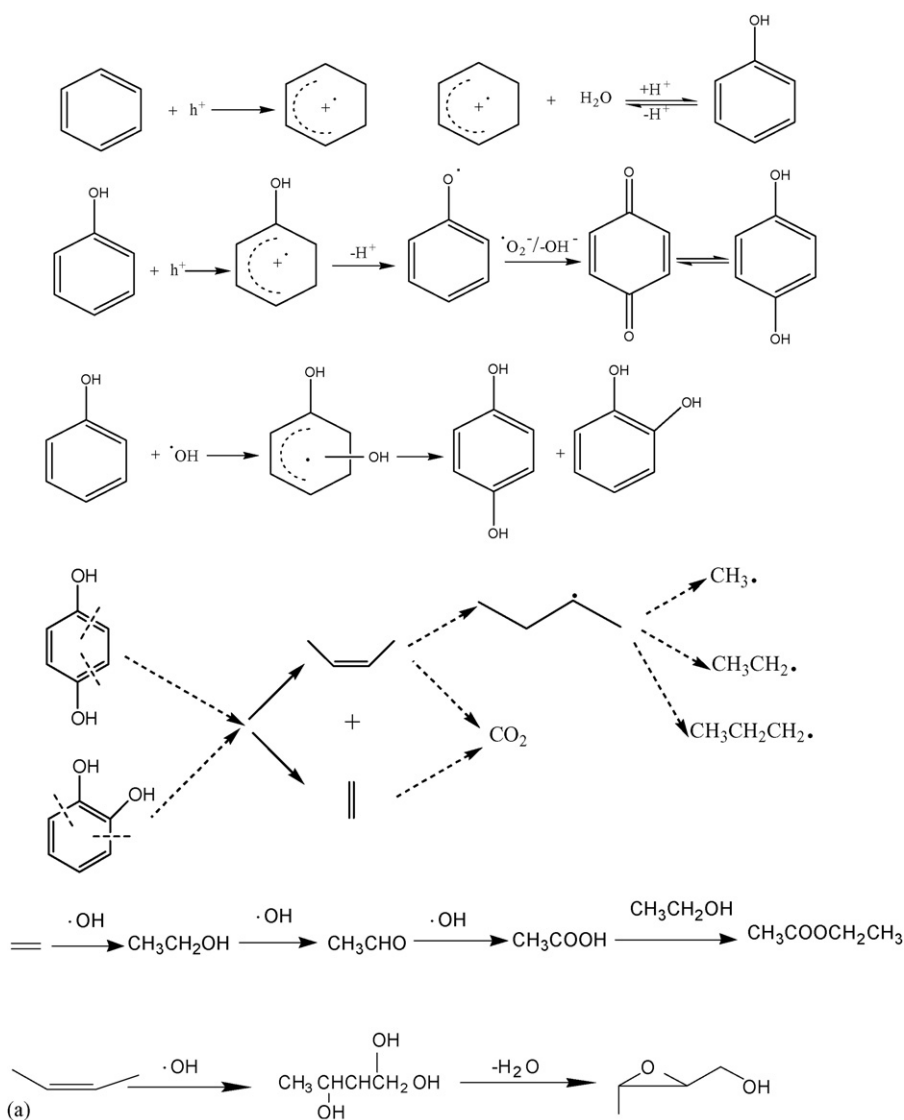No intermediates were detected in the gas phase under the conditions.

Fig. 10. Photocatalytic oxidation mechanism of benzene: (a) primary benzene photocatalytic oxidation mechanism; (b) secondary benzene photocatalytic oxidation mechanism.
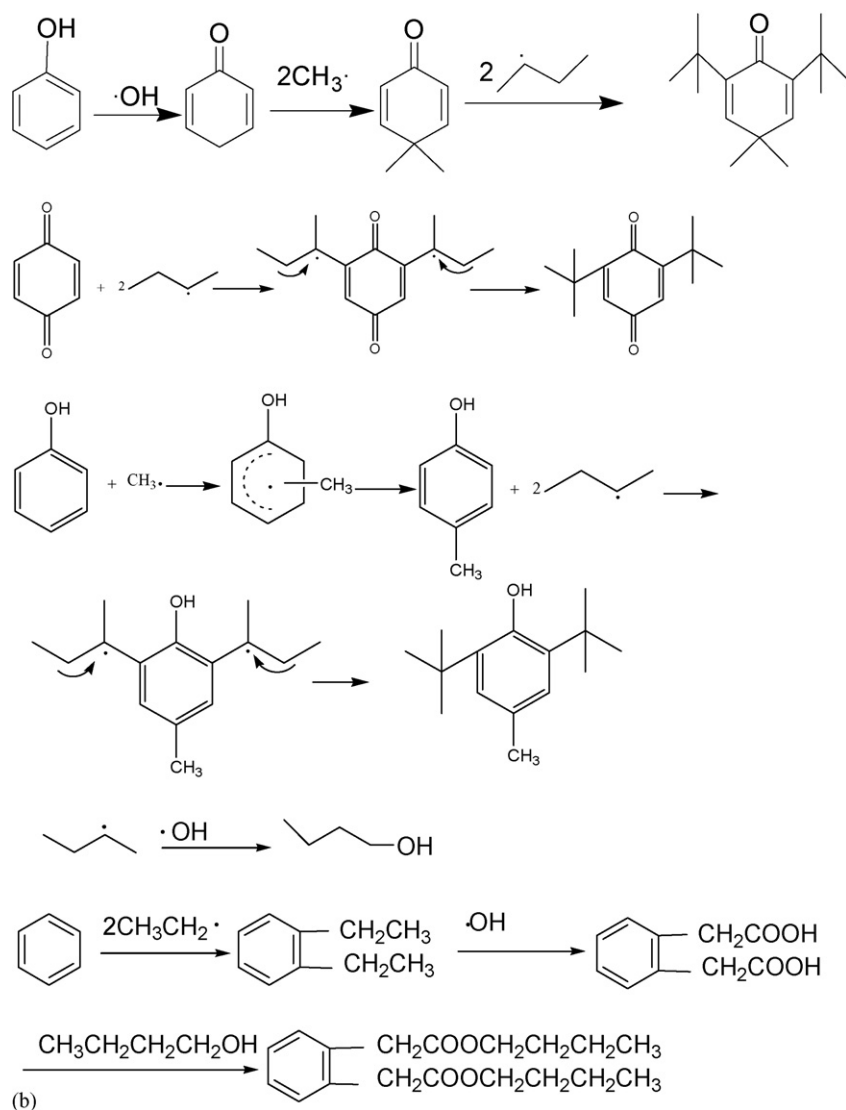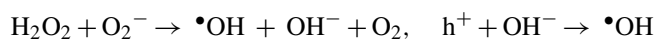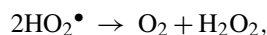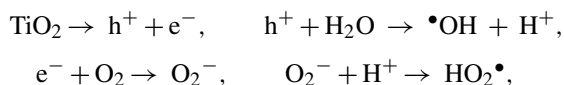
Fig. 10. (*Continued*).

Following photocatalyzed benzene destruction in air, the deactivated TiO_2/Sr_2CeO_4 was ultrasonicated in ether and the resulting solution was evaporated to concentrate any dissolved intermediates, then the concentrated solution was analyzed by GC/MS for intermediates. Figs. 8 and 9 show the chromatograms of the intermediates from TiO_2/Sr_2CeO_4 and TiO_2 detected by GC/MS. The detected compounds included: (1) ethyl acetate; (2) benzene; (3) (3-methyl-oxiran-2-yl)-methanol; (4) 2,6-bis(1,1-dimethylethyl)-4,4-dimethylycyclohe; (5) 2,5-cyclohexadiene-1,4,dione,2,6-bis(1,1-dim); (6) butylated hydroxytoluene; (7) dibutyl phthalate.

As shown in Figs. 8 and 9, the main intermediate is (3-methyl-oxiran-2-yl)-methanol and ethyl acetate.

Based on the reaction products identified, the photocatalytic oxidation mechanism of benzene in air was speculated and depicted in Fig. 10:

$$TiO_2 \rightarrow h^+ + e^-, \qquad h^+ + H_2O \rightarrow {}^\bullet OH + H^+,$$

$$e^- + O_2 \rightarrow O_2{}^-, \qquad O_2{}^- + H^+ \rightarrow HO_2{}^\bullet,$$

$$2HO_2{}^\bullet \rightarrow O_2 + H_2O_2,$$

$$H_2O_2 + O_2{}^- \rightarrow {}^\bullet OH + OH^- + O_2, \quad h^+ + OH^- \rightarrow {}^\bullet OH$$

In the experimental conditions, the main intermediates are ethyl acetate and (3-methyl-oxiran-2-yl)-methanol on both photocatalysts. As shown in Fig. 9, the primary benzene photocatalytic oxidation mechanisms on both photocatalysts are the same, while there is a difference between secondary benzene photocatalytic oxidation mechanisms.

d'Hennezel and co-workers reported the major by-products of benzene was phenol which was accompanied by hydroquinone and 1,4-benzoquinone [5],while Jacoby et al. noted that the formation of be phenol, maloinic acid, hydroquinone, benzoic acid and benzoquinone in the case of benzene photocatalytic oxidation [18,19]. Zhang investigated the IR spectrum of the deactivated catalyst, their results showed the intermediate product was a hexatomic ring alcohol [29]. Based on the above different results, we can draw a conclusion that the gas-phase photocatalytic oxidation of benzene

have different reaction mechanisms under different reaction conditions.

Many authors [30,31] argued that the deactivation of catalyst could be attributed to the two following reasons: (1) the surface active sites were occupied by the less-reactive poisonous intermediates; (2) surface hydroxyl groups were consumed. In our experimental conditions, compared with TiO_2/Sr_2CeO_4 used 2 h, on the deactivated photocatalyst surface appeared three less-reactive intermediates: 2,5-cyclohexadiene-1,4,dione, 2,6-bis(1,1-dim), butylated hydroxytoluene and 2,6-bis(1,1-dimethylethyl)-4,4-dimethylycyclohe, it is plausible that at least one of these less-reactive intermediates caused the deactivation of the photocatalyst, which could be supported by the fact that the color of catalyst turned from white to yellow during the reaction process.

4. Conclusion

The paper revealed that the degradation of gaseous benzene was a pseudo first-order reaction, and Langmuir–Hinshewood kinetic model was successfully applied to describe this process. Mathematic inference showed that the limiting rate constant and the adsorption constant in this case were $0.0064\,mg\,l^{-1}\,min^{-1}$ and $9.2078\,l\,mg^{-1}$, respectively. By using FT-IR spectroscopy we have identified the main partial oxidation products formed on the surface of deactivated catalyst. Additionally, GC/MS analysis of ether-extracted surface species confirmed the presence of (3-methyl-oxiran-2-yl)-methanol and ethyl acetate and detected small concentrations of 2,6-bis(1,1-dimethylethyl)-4,4-dimethylycyclohe, 2,5-cyclohexadiene-1,4,dione, 2,6-bis(1,1-dim) and butylated hydroxytoluene. These species appears to be less reactive than benzene, it is plausible that at least one of the three less-reactive intermediates caused the deactivation of the photocatalyst. Based on the results, the degradation mechanisms were speculated.

References

[1] S.B. Kim, S.C. Hong, Kinetic study for photocatalytic degradation of volatile organic compounds in air using thin film TiO$_2$ photocatalyst, Appl. Catal. B: Environ. 35 (2002) 305–315.

[2] J. Zhao, X.D. Yang, Photocatalytic oxidation for indoor air purification: a literature review, Build. Environ. 38 (2003) 645–654.

[3] T.K. Kim, M.N. Lee, S.H. Lee, Y.C. Park, C.K. Jung, J.H. Boo, Development of surface coating technology of TiO$_2$ powder and improvement of photocatalytic activity by surface modification, Thin Solid Films 475 (2005) 171–177.

[4] W. Wang, Y. Ku, Photocatalytic degradation of gaseous benzene in air streams by using an optical fiber photoreactor, J. Photochem. Photobiol. A: Chem. 159 (2003) 47–59.

[5] O. d'Hennezel, P. Pichat, D.F. Ollis, Benzene and toluene gas-phase photocatalytic degradation over H$_2$O and HCL pretreated TiO$_2$: by-products and mechanisms, J. Photochem. Photobiol. A: Chem. 118 (1998) 197–204.

[6] N.N. Lichtin, M. Sadeghi, Oxidative photocatalytic degradation of benzene vapor over TiO$_2$, J. Photochem. Photobiol. A: Chem. 113 (1998) 81–88.

[7] W. Wang, L.W. Chiang, Y. Ku, Decomposition of benzene in air streams by UV/TiO$_2$ process, J. Hazard. Mater. B 101 (2003) 133–146.

[8] H. Einaga, S. Futamura, T. Ibusuki, Heterogeneous photocatalytic oxidation of benzene, toluene, cyclohexene and cyclohexane in humidified air: comparison of decomposition behavior on photoirradiated TiO$_2$ catalyst, Appl. Catal. B: Environ. 38 (2002) 215–225.

[9] W.K. Jo, K.H. Park, Heterogeneous photocatalysis of aromatic and chlorinated volatile organic compounds (VOCs) for non-occupational indoor air application, Chemosphere 57 (2004) 555–565.

[10] X.Z. Fu, W. Zeltner, M.A. Anderson, The gas-phase photocatalytic mineralization of benzene on porous titania-based catalysts, Appl. Catal. B: Environ. 6 (1995) 209–224.

[11] O. d'Hennezel, D.F. Ollis, Trichloroethylene-promoted photocatalytic oxidation of air contaminants, J. Catal. 167 (1997) 118–126.

[12] T. Hisanaga, K. Tanaka, Photocatalytic degradation of benzene on zeolite-incorporated TiO$_2$ film, J. Hazard. Mater. B 93 (2002) 331–337.

[13] M. Lewandowski, D.F. Ollis, A two-site kinetic model simulating apparent deactivation during photocatalytic oxidation of aromatics on titanium dioxide (TiO$_2$), Appl. Catal. B: Environ. 43 (2003) 309–327.

[14] K.I. Shimizu, H. Akahane, T. Kodama, Y. Kitayama, Selective photooxidation of benzene over transition metal-exchanged BEA zeolite, Appl. Catal. A: Gen. 269 (2004) 75–80.

[15] J.F. Wu, C.H. Hung, C.S. Yuan, Kinetic modeling of promotion and inhibition of temperature on photocatalytic degradation of benzene vapor, J. Photochem. Photobiol. A: Chem. 170 (2005) 299–306.

[16] H.W. Park, W.Y. Choi, Photocatalytic conversion of benzene to phenol using modified TiO$_2$ and polyoxometalates, Catal. Today 101 (2005) 291–297.

[17] G.M. Zuo, Z.X. Cheng, H. Chen, G.W. Li, T. Miao, Study on photocatalytic degradation of several volatile organic compounds, J. Hazard. Mater. B 128 (2006) 158–163.

[18] G.B. Raupp, T.C. Junio, Photocatalytic oxidation of oxygenated air toxics, Appl. Surf. Sci. 72 (1993) 321–327.

[19] W.A. Jacoby, D.M. Nlake, J.A. Fennell, J.E. Boulter, L.M. Vargo, M.C. Geroge, S.K. Dolberg, Heterogeneous photocatalysis for control of volatile organic compounds in indoor air, J. Air Waste Manage. Assoc. 46 (1996) 891–898.

[20] J. Blanco, P. Avila, A. Bahamonde, E. Alvarez, B. Sanchez, M. Romero, Photocatalytic destruction of toluene and xylene at gas phase on a titania based monolithic catalyst, Catal. Today 29 (1996) 437–442.

[21] M. Toshiyuki, C. Takanobu, I. Nobuhito, G.Y. Adachi, Synthesis and luminescence of Sr$_2$CeO$_4$ fine particles, Mater. Res. Bull. 38 (2003) 17–24.

[22] F. Shi-Liu, D. Jun, Z.F. Fang, Synthesis of Sr$_2$CeO$_4$ phosphor by mechanical and reactive sintering, Chin. J. Inorg. Chem. 20 (2004) 698–702.

[23] J.G. Yu, X.J. Zhao, Q.N. Zhao, J.C. Du, XPS of study of TiO$_2$ photocatalytic thin film prepared by the sol–gel method, Chin. J. Mater. Res. 14 (2000) 203–209.

[24] Y.X. Tang, H.P. Guo, Q.Z. Qin, Photoluminescence of Sr$_2$CeO$_4$ phosphors prepared by microwave calcination and pulsed laser deposition, Solid State Commun. 121 (2002) 351–356.

[25] A. Bouzaza, A. Laplanche, Photocatalytic degradation of toluene in the gas phase: comparative study of some TiO$_2$ supports, J. Photochem. Photobiol. A: Chem. 150 (2002) 207–212.

[26] C. Raillard, V. Héquet, P.L. Cloirec, Legrand, Kinetic study of ketones photocatalytic oxidation in gas phase using TiO$_2$-containing paper: effect of water vapor, J. Photochem. Photobiol. A: Chem. 163 (2004) 425–431.

[27] R.M. Alberici, W.F. Jardim, Photocatalytic destruction of VOCs in the gas-phase using titanium dioxide, Appl. Catal. B: Environ. 14 (1997) 55–68.

[28] C.H. Ao, S.C. Lee, J.Z. Yu, J.H. Xu, Photodegradation of formaldehyde by photocatalyst TiO$_2$: effects on the presences of NO, SO$_2$ and VOCs, Appl. Catal. B: Environ. 54 (2004) 41–50.

[29] Q.C. Zhang, F.B. Zhang, G.L. Zhang, Reaction mechanism of gas-phase photocatalytic oxidation of benzene on TiO$_2$, Chin. J. Catal. 25 (2004) 39–43.

[30] C. Xie, Z.L. Xu, Q.J. Yang, N. Li, D.F. Zhao, D.B. Wang, Y.G. Du, Comparative studies of heterogeneous photocatalytic oxidation of heptane and toluene on pure titania, titania–silica mixed oxides

and sulfated titania, J. Mol. Catal. A: Chem. 217 (2004) 193–201.

[31] G. Marci, M. Addamo, V. Augugliaro, S. Coluccia, E.G. Lopez, V. Loddo, G. Martra, L. Palmisano, M. Schiavello, Photocatalytic oxidation of toluene on irradiated TiO_2: comparison of degradation performance in humidified air, in water and in water containing a zwitterionic surfactant, J. Photochem. Photobiol. A: Chem. 160 (2003) 105–114.